Single-Layer Series-Fed Planar Array with Controlled Aperture Distribution for Circularly Polarized Radiation

Single-Layer Series-Fed Planar Array with Controlled Aperture Distribution for Circularly Polarized Radiation

Pascual D. Hilario Re, Davide Comite, and Symon K. Podilchak

***Abstract*—We propose a compact circularly polarized series-fed patch array with enhanced radiation performance at S-band. To our best knowledge, no similar single-layer structure has been designed, measured and reported in the literature with equivalent radiation performances in terms of reduced sidelobe-level (SLL) and aperture efficiency as well as compactness and simplicity. The planar array consists of a 50-Ω microstrip single feed point, offering uniform and efficient excitation of all its elements that enables a broadside beam with high-gain and low sidelobes. A feed network for such aperture control is designed and optimized to provide good impedance matching with a two-point excitation per radiating element, which is based on 0° and 90° meander lines to enable circularly polarized radiation. A structure made by a 4×1 arrangement of square patches is simulated, optimized, and manufactured, providing a realized gain of about 10 dBic and a SLL below -15 dB. Very good axial ratios and high efficiencies are obtained. The proposed antenna may be of interest for next-generation far-field wireless power transmission systems and other applications including target tracking, radar and internet of things technologies requiring efficient circularly polarized radiation.**

***Index Terms*—Controlled aperture distribution, series-fed array, circular polarization, radar, wireless power transfer.**

I. Introduction

Thanks to their reduced weight and cost, one-dimensional and two-dimensional arrays of planar antennas are considered conventional solutions to achieve high-gain and good side-lobe levels (SLLs) [1]. In the last few decades, various shaped microstrip patch antennas have been introduced, mostly thanks to their low-profile nature and capability to achieve circular polarization (CP) by means of single feeds [2]–[9]. The simplest solution to excite these structures consists in the use of fully integrated planar feed networks, which can be properly designed to achieve frequency scanning high-gain beams or broadside radiation within a certain bandwidth (BW).

As it is well-known, a feeding network is needed to control amplitude and phase distribution at each element of the array, which is typically achieved by means of two alternative configurations, i.e., corporate and series feeds, which can be arranged on single or multi-layer structures [1]. The latter is based on a single transmission line that progressively couples power to each element of the array. With respect to the corporate feed it allows for the possible reduction in the size of the network and the number of feed lines, an aspect that can be highly desirable to maximize the array efficiency and to minimize the SLLs [10]. This is typically achieved, however, at the expense of a narrow operational BW, and it requires phase synchronization to compensate for the inherent phase difference between the array elements. In both cases, the feeding network should be optimized to minimize interferences with radiation from the array. In this frame, circular polarized beams can be obtained either by using CP radiating elements [11], [12], or by a composite layout in which more antennas are properly arranged with the required magnitude and phase [13], [14]. In general, the latter method limits the possibilities of using the configuration of the radiating elements to shape the array pattern.

Manuscript received July 3rd, 2019. This work was supported by Samsung under the GRO Grant Scheme as well as European Union's Horizon 2020 Research and Innovation Programme under the Marie Skłodowska Curie Project CSA-EU under Grant 709372.

Pascual D. Hilario Re and Symon K. Podilchak are with The University of Edinburgh and Heriot-Watt University, Edinburgh, Scotland, UK (e-mail: skp@ieee.org)

Davide Comite is with the Department of Information Engineering, Electronics and Telecommunications, "Sapienza" University of Rome, 00184 Rome, Italy (davide.comite@uniroma1.it).

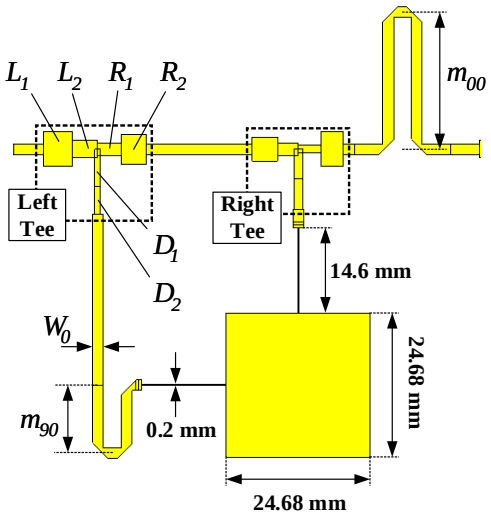

Fig. 1. Antenna element within the array: left and right tees are introduced to control the amplitude distribution, while 90° and 0° meander delay lines, with vertical line lengths defined by m_{90} and m_{00}, respectively (and a common width of W_0), are optimized for proper quadrature phasing, excitation of the square patch and inter-element phase synchronization. Also, each tee is defined by six independent transmission lines that are optimized to achieve the desired power split (L_1, L_2, R_1, R_2, D_1, D_2).

We propose here a uniformly excited CP microstrip array defined by a series feeding technique that allows for control and tunning of the amplitude and phase distribution at each element within the array for quadrature excitation. Our approach enables other controlled aperture distributions and tapering for efficient radiation and with low SLLs compared to other CP series-fed arrays. In fact, to the authors' best knowledge, no similar CP antenna array has been reported based on such a simple design through a 50-Ω microstrip transmission line connected to a single input port and with uniform excitation of its elements. In particular, a high-gain broadside beam, reaching a realized gain in excess of 9.8 dBic, is observed. A detailed comparison with other works in the literature is reported, demonstrating that the proposed structure offers improved performance in terms of efficiency and SLLs (-15 dB) while maintaining reduced costs, compact size, design simplicity, ease of fabrication and full integrability with other planar single-layer structures. Possible applications could include retrodirective antenna technologies, wireless power transmission, radar, and other single-frequency tracking systems.

II. Single Element Design

We firstly report here the design of the elements within the array at 2.4 GHz, whose geometric configuration and feeding points are optimized to achieve high CP purity and compactness. The

approach can generally be applied to patches of arbitrary shape, but for simplicity, we consider a conventional squared microstrip patch antenna [1]. Two designs based on different commercial substrates are considered, i.e., a RO3206 substrate from Rogers with thickness $h = 1.27$ mm, relative permittivity $\varepsilon_r = 6.15$, and loss tangent $\tan\delta = 0.0027$, and a TLY5 Taconic with $\varepsilon_r = 2.18$, $h = 1.57$ mm, and $\tan\delta = 0.0009$. A substrate about 20% thinner is chosen in the first case to limit dielectric losses.

The dimension for both sides of the patch for the Rogers and the Taconic substrate are 24.7 mm and 40.6 mm, respectively. This makes the patch printed on the Rogers substrate to be 40% smaller due to the difference in the relative permittivity between the two laminates. Quarter-wave transformers are connected to the patch edges to feed the elements with a 90° phase difference between the relevant ports, as needed for CP radiation (see Fig. 1 for the schematic of the single-element). The structure is simulated and optimized with CST Microwave studio.

Considering 4 elements within the array and with ideal feeding, i.e., a 4×1 array, simulations for the realized gain over frequency show a -3 dB radiating BW of about 3%, which might be suitable for several applications such as wireless power transmission (WPT) in the far-field, retrodirective antenna arrays, or radar where efficient and low-cost PCB structures are needed. Due to the different laminates, the maximum realized CP gain of the two prototypes differs by about 2 dB (all results not shown for brevity).

The axial ratio (AR) for both designs are below 0.7 dB in the entire simulated band (2 to 3 GHz), confirming highly pure CP operation. Also, the patterns demonstrate good CP radiation versus angle, exhibiting a 180° AR beamwidth (BMW) less than 3 dB in both principal planes. For the aforementioned Rogers design, in terms of realized gain versus angle, the 3 dB BMW is approximately 98° in both planes. Similar CP radiation values were observed for the Taconic substrate.

The total radiation efficiencies at 2.4 GHz for the two structures (which includes ohmic losses and reflection losses), are equal to about 73% for the Rogers and 86% for the Taconic substrate. As expected, the larger value of ε_r leads to a reduced efficiency, mainly due to the $\tan\delta$ of 0.0027 for the RO3206 substrate. However, increasing the permittivity of the substrate allows for a reduction in the antenna size, and, therefore, the possibility of reducing the distance between the array elements to avoid high sidelobes as well as to accomodate the spacing requirements for the feed system. To enhance the radiation features when implementing the array, at the expense of an acceptable loss of efficiency while maintaining compactness, we consider in the following sections the RO3206 laminate.

III. Array Feed Design

The single-element described in the previous section is employed here to design a series-fed 4×1 CP array excited by means of a single feed line using microstrip technology. To achieve persistent high-gain broadside radiation, the feeding amplitude and phase are properly controlled at each array element by ensuring an uniform distribution; i.e., we adopt an equal amplitude excitation for each radiating element. Hence meanders and impedance transformers for phase and amplitude control, respectively, are introduced and optimized. On this basis, standard transmission-line theory [15] is used to evaluate the input impedance of the antenna and to control the relevant phase offset at 2.4 GHz for CP radiation. The corresponding network dimensions vary from 0.2 mm to 10 mm in width, and from 1 mm to 20 mm in length. A schematic view of the unit cell for the single element and an illustration of the feeding network is reported in Figs. 1 and 2.

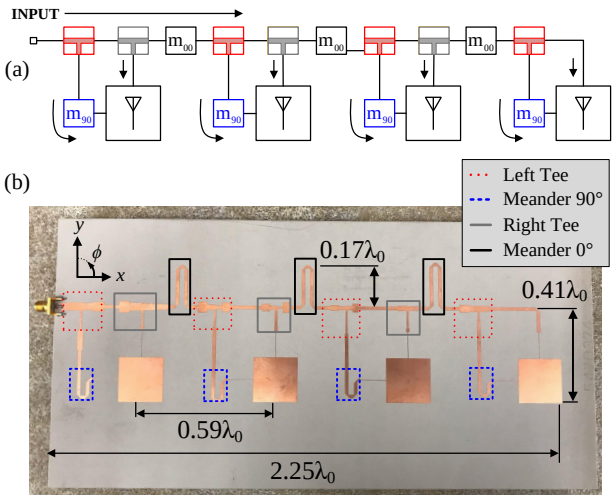

Fig. 2. Block diagram (a) that divides each antenna element into four parts: left tee (shown in red), which provides a -9 dB of power diversion towards the horizontal feed; meander 90° (blue), which provides the 90° offset between orthogonal antenna feeds; right tee (yellow), providing the -9 dB of power diversion towards the vertical feed; meander 0° (black), responsible for the in-phase excitation between all the patch elements, and (b) photograph of the proposed sub-array design. Specific dimensions can be found in Table I.

As it is visible, the left and right *tees* control the power distribution at the input of each of the patch edges as well as the power injected towards the adjacent antenna element. Each tee is made by two independent transmission lines per branch (i.e, L_1, L_2, D_1, D_2, R_1 and R_2). The meanders also have a constant width, given by W_0, and include chamfered corners on each of the 90° turns to minimize undesired reflections caused by capacitive effects arising at the corners [15], [16].

Additionally, in Fig. 1, m_{90} indicates the meander section that controls the phase offset between the antenna ports, whereas m_{00} provides connectivity between all array elements. The length of the horizontal transmission line of all meanders is fixed to 5 mm, being a compromise between the need for compactness and the mitigation of the coupling between the arms of the meander.

A full-wave procedure was then implemented to optimize the performance of the feeding network. During the full-wave simulation steps the amplitude balance was firstly tuned, followed, secondly, by a fine adjustment of the meanders length to find the relevant phase balance. Finally, an additional optimization step was performed to introduce a very small refinement of the transmission lines widths, and to compensate for the small impedance variations introduced during the second step. The geometric dimensions of the optimized network are reported in Table I. No values are reported for the right tee of the last antenna element, since all the power reaching this point goes to the top port of the last patch.

Figure 2 presents a picture of the manufactured series-fed array. The first meander line (blue box), controls the phase difference of the orthogonal modes supported by the antenna element, while the second (black box), the phase difference. As regards the amplitude distribution, uniform weights have been applied to each patch. Hence, two impedance transformers are positioned at the tee junctions to provide the same power at the two network branches. The spacing between the antenna elements has been finely tuned, which for the final configuration is equal to $0.59\lambda_0$.

To quantify the effects on the array performance introduced by the feeding system, in terms of radiation and total efficiency, we have studied the antenna in the absence of feeding network. A

TABLE I
DIMENSIONS (IN MM) OF THE FEEDING NETWORK FOR THE PROPOSED SERIES-FED CP ARRAY

	A_1				A_2				A_3				A_4			
	Left tee		Right tee		Left tee		Right tee		Left tee		Right tee		Left tee		Right tee	
	L	W	L	W	L	W	L	W	L	W	L	W	L	W	L	W
L_1	5.86	4.01	5.82	6.5	4.93	6	4.36	4.1	4.66	3	6.65	2.03	5.28	4.12	-	-
L_2	6.81	4.46	6.8	4.26	3.89	3.04	2.81	2.14	3.82	2.1	4.89	2.89	4.75	3.21	-	-
R_1	6.5	4	7.83	3.78	3.49	2.09	3.06	1.24	2.9	2.35	4.58	2.38	5.53	3.11	-	-
R_2	5.86	5.5	6.76	3	4.38	5.13	3.77	6	3.24	4.96	0.38	2.93	5	1.8	-	-
D_1	11	1	4.14	1	4.95	1	4	1.5	7	1	5.15	1	4.2	1	-	-
D_2	11	3	4.05	1	4.72	1	5.25	1.5	6.5	1	4.71	1	2	1.5	-	-
m_{90}	10				11.65				9.1				8.1			
m_{00}	20.87				21.6				23.33				-			
W_0	1.83															

degradation of the radiation and total efficiencies of about 8% and 9%, respectively, has been observed (complete results not reported for brevity). An improvement of 1.2 dB for the SLL in the presence of the network is also visible, but no significant variation of the realized gain has been observed. To summarize, the feed system has a minor and acceptable impact on the radiation performance of the CP array.

The amplitude and phase balances at each element within the array are also investigated to assess the microstrip feeding network. This simulation model is shown in Fig. 3 while results are reported in Figs. 4 and 5. Around 2.4 GHz, an amplitude variation of the S-parameters within 1 dB can be observed (note that, given the 4×1 array layout and uniform element excitation, a power split of -9 dB is required for each port), thus resulting in about 1 dB of insertion losses. The phase balance (see Fig. 5) exhibits good CP feeding to each of the four patches at the design frequency which ensures quadrature excitation within a tolerance of $90° \pm 2°$.

IV. SERIES-FED ARRAY PERFORMANCE

The measured and simulated reflection coefficients for the series-fed patch array are reported in Fig. 6 and a good agreement is observed around the design frequency, which is zoomed in the figure inset. A minor frequency shift can be observed for the reflection coefficient and this is likely related to the manufacturing tolerance for the relative permittivity of the employed substrate. To further understand this practicality, new simulations were completed to estimate the value of ε_r. Results suggest that the actual relative permittivity, defining the employed RO3206 substrate, was actually 6.32 and not the rated value of 6.15. This is clearly shown in Fig. 6 where an excellent agreement can be observed between the simulations (with $\varepsilon_r = 6.32$) and the measurements.

These results further suggest that the center frequency for the series-fed array is slightly lower than originally intended. In fact, results in the inset of Fig. 6 clearly show that the center frequency for the fabricated structure was about 2.37 GHz and not 2.4 GHz as per the original design. This can be seen by inspecting the minimum of the $|S_{11}|$ plot, which is below -20 dB at about 2.37 GHz for the measured structure. It should also be mentioned that the mutual coupling between the patch elements has been studied during the optimization of the array and its feeding network. Coupling values below -20 dB (not shown for brevity) have been achieved, suggesting that the mutual coupling between elements is properly considered.

Far-field simulations in Fig. 7 further suggest that there is a very minor difference in array performance due to this frequency shift. It can be observed that the value for the maximum realized gain, the beam pattern shape and its pointing angle, as well as the cross-polarization level, are consistent, albeit the shift in center frequency for the array. The realized CP gain at broadside is reported in Fig. 8 versus frequency as well as the cross-polarization levels. In addition, the AR versus frequency and the AR BMW is plotted in Fig. 9 where

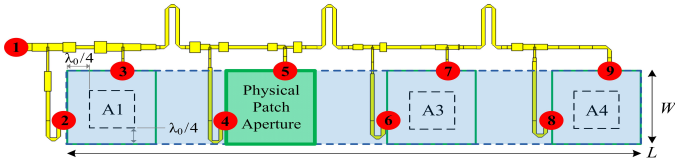

Fig. 3. Schematic view of the optimized series-fed feeding system where the input of the array is at port 1. A controlled aperture distribution along the array, with uniform amplitude excitation for CP, is achieved through the series network of meandered transmission lines and impedance transformers where antenna elements are labeled left to right; i.e. $A1$, $A2$, $A3$, and $A4$. The physical aperture size for the array, which extends $\lambda_0/4$ beyond the physical edges of the exterior patch elements, $A1$ and $A4$, is defined as $L \times W$.

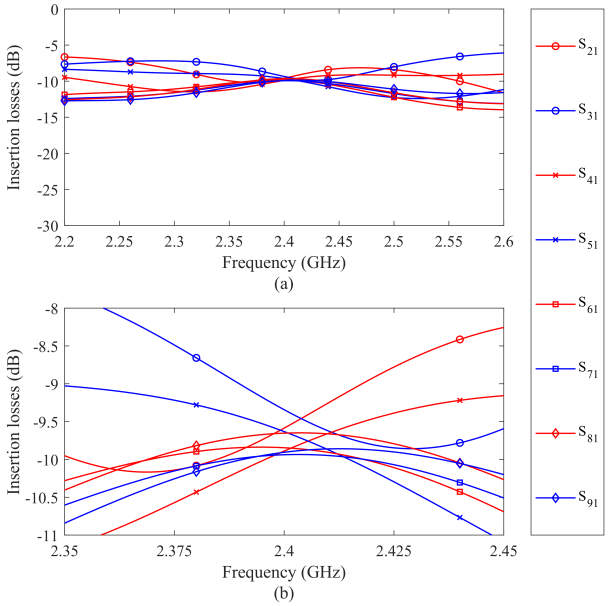

Fig. 4. Simulated amplitude balance for the optimized feed system shown in Fig. 3: (a) S-parameter response and (b) zoomed view around 2.4 GHz. It can be observed that at the design frequency, all elements are fed with about the same amount of input power.

agreement can be observed in the measurements and simulations. Figures 10 and 11 report the simulated and measured realized gain at 2.37 GHz in the principal planes. Good SLLs (around -15 dB) are observed. Finally, Figs. 12 and 13 present the realized gain at 2.38 GHz, showing good cross-polarization levels and high-gain.

The simulated and measured AR versus frequency and angle is shown in Fig. 9. Also, the AR measurements in both cases (a-b) appear degraded if compared to the simulations. This is likely caused

TABLE II
COMPARISON TO OTHER SERIES-FED CP ARRAYS FOUND IN THE LITERATURE

	Array Type	Frequency (GHz)	Antenna Length (λ_0)	Element Spacing (λ_0)	Imp. BW (%)	Realized Gain, G (dBic)	3 dB AR BMW (deg.) ϕ = 0 / 90°	AR BW (%)	AR Min. (dB)	First SLL (dB)	Single or Multi-layer	Aperture Control or Tapering	Aperture Efficiency (%)
[8]$^{\diamond}$	6×2	6.83, 7.14	4.1, 4.3	0.56, 0.53	7.9, 6.58	15.9, 16.3	-	3.2, 4.3	0.9, 0.6	-9, -7	S	E	49.4†55.5†
[11]	1×5	5.6	4.6	0.91	12	12.4	20 / -	-	2.2	-11	S	E	35.6†
[17]	1×12	8	6	0.46	5	12.5	50 / -	-	3.9	-10.5	S	E	32.5†
[18]	1×12	8	6	0.46	5	12	45 / -	12.8	1.1	-10.5	S	E	21.6†
[19]	1×10	10.5	5	0.5	4	15.94	12.5 / -	3.1	2.5	-12.34	M	E	46.3†
[20]$^{\diamond}$	1×24	260	11.2	0.42	3.85	15.32	25 / 50	-	1.27	-12.5	M	E	22.7†
[21]*	1×4	17.5	3.4	0.68	7.4	9.36	110 / -	1.6	1.6	-13.5	M	E	70.0 / 28.5
[22]*	1×5	3	4	0.67	8.5	-	30 / -	9.3	0.2	-22	S	C	-
[23]$^{\natural}$	1×8 SR	10	1.33	0.51	15	11.1	55 / 90	15.7	1.2	-11.5	M	E	28.1 / 29.7
This work	1×4	2.37	2.4	0.59	1.8	9.8	40 / 64	0.4	2.3	-15.1	S	U	43.9†

Table Acronyms: Single-layer (S), Multi-layer (M), Exponential (E), Chebyshev (C), and Uniform (U).

† Aperture efficiency calculated using $G\lambda_0^2/(4\pi A_{\text{phys}})$ [1], where G is the measured CP realized gain in linear units, λ_0 is the free-space wavelength, and A_{phys} $(= L \times W)$ corresponds to the physical rectangular aperture area (see Fig. 3), which has been estimated by adding $\lambda_0/4$ to each of the four sides of the array.

$^{\diamond}$ Antenna results for [8] and [20] are based on simulations only. All other values in this table are defined by the fabricated arrays and measurements.

* First value for the aperture efficiency for [21] has been calculated by considering just the area of the substrate. This is because in [21], the size of the array printed on the substrate is physically smaller then when adding $\lambda_0/4$ to each of the sides. For a fair comparison, the second value of the aperture efficiency has been obtained following the procedure described above† which uses an area of the physical aperture, in this case, which is larger than the PCB itself.

* No aperture efficiency value is calculated in this table for [22] since no CP realized gain values were reported.

$^{\natural}$ [23] reports a circular array with sequential rotation (SR). For a fair comparison, the physical aperture was calculated using a circle with a radius defined by the outer edges of the radiating elements for the array, but with a radius enlarged by $\lambda_0/4$. This circular area, A_{C1}, was used to calculate the first value for the aperture efficiency estimation. The second aperture efficiency value was obtained by considering the circular area A_{C2} (given by a circle with radius defined by the inner edge of the radiating elements minus $\lambda_0/4$) subtracted from A_{C1}.

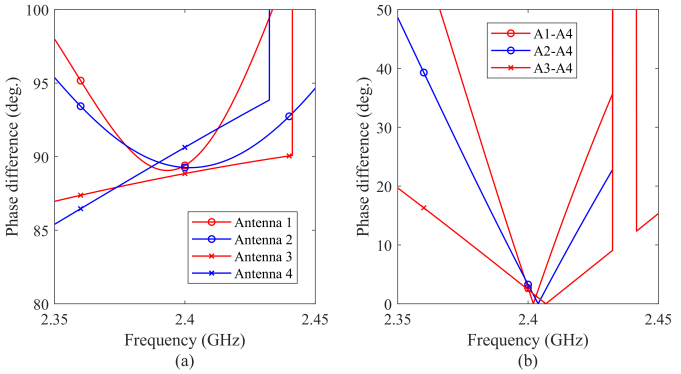

Fig. 5. Simulated phase balance of the feed system: (a) phase difference considering the same element (see Fig. 3); (b) phase difference between elements. Results show that the each antenna element within the array is driven in quadrature at 2.4 GHz.

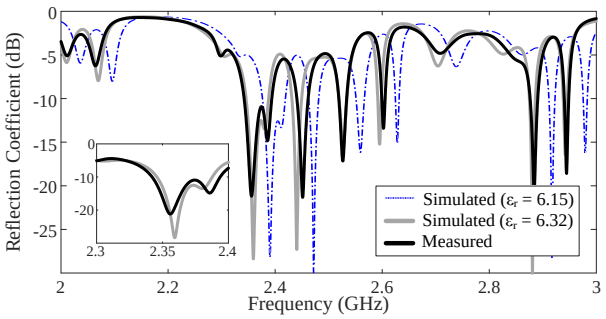

Fig. 6. Reflection coefficient for the proposed series-fed CP array from 2 to 3 GHz and from 2.3 to 2.4 GHz in the inset. Results show a very good agreement between the measurements and simulations considering ϵ_r = 6.32 (black dashed line) over the frequency band. It should be mentioned that initially simulations were performed considering ϵ_r = 6.15 (blue dashed line), but after measuring the manufactured prototype, a shift in the resonant frequency was observed which suggests actually ϵ_r = 6.32. This can be related to tolerances in the relative permittivity for the employed substrate.

by some small alignment errors during the measurements and by using a practical reference antenna which did not have ideal cross-polarization levels. Regardless, the AR is about 2 dB at the antenna design frequency, while the 3−dB AR BMW is 40° and 64° in the ϕ = 0° and ϕ = 90° principal planes, respectively.

To better assess the features of the proposed CP array with uniform excitation of its elements, we report in Table II a comparison with other series-fed CP arrays found in the literature. It can be observed that the proposed series-fed CP array provides a compromise between antenna compactness, best possible SLLs given the employed uniform aperture distribution (which has not been demonstrated previously), and antenna aperture efficiency. Approaches to characterize and mathematically optimize such a series-fed array in terms of the minimization of the AR over a specified frequency bandwidth can be found in [7] whilst also considering the impedance BW.

Although the proposed array provides narrow-band operation (as also observed with other series-fed CP arrays, see Table II), the low SLLs and the CP radiation achieved with the simple design (only 4 compact elements), make it an excellent candidate for applications such as far-field wireless power transfer, radar or satellite communications. It should also be mentioned that this performance has been achieved avoiding feeding networks made by multiple transmission lines as well as dual- or multi-layer laminates, which can significantly

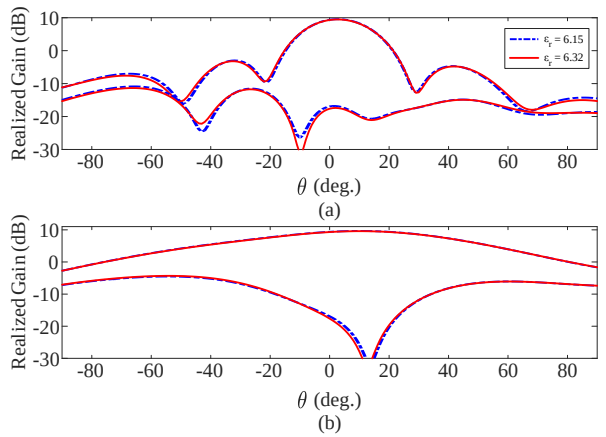

Fig. 7. Simulated realized gain with ϵ_r = 6.32 and 6.15 for the modeled substrate at 2.37 and 2.40 GHz, respectively; (a): x-z-plane (ϕ = 0°), (b): y-z-plane (ϕ = 90°). Cross-polarization levels are also shown.

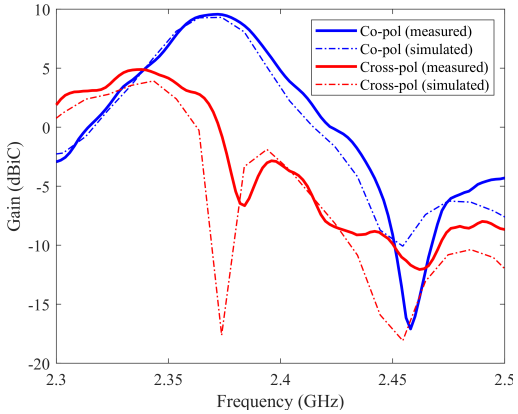

Fig. 8. Realized gain versus frequency for the proposed series-fed CP array. Cross-polarization levels are also shown. A good agreement is observed since the simulations consider $\varepsilon_r = 6.32$ for the substrate.

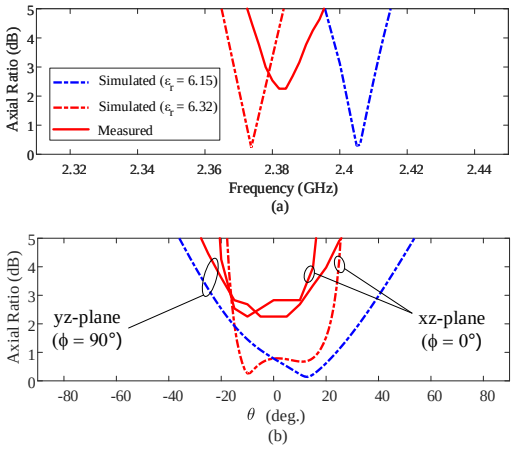

Fig. 9. Measured and simulated AR considering ϵ_r = 6.15 and 6.32 for the series-fed array: (a) AR versus frequency at antenna boresight; (b) simulated AR versus the zenith angle and compared to measurements at 2.38 GHz.

increase the complexity in the fabrication process of the array as well as increase the size of the antenna.

We should also mention that the use of metamaterial transmission lines could further enhance the performance of the proposed feeding network, as discussed, e.g., in [24], [25], where, however, linearly polarized devices are considered, and are therefore not directly comparable with our proposed design. For simplicity, uniform excitation of the patches has been considered in our design. This opens up the possibility to further decrease the SLL and control the beam pattern, in particular, by tapering the array using alternative approaches (such as binomial, Chebychev, or cosine-squared, etc.) as well as increasing the number of CP elements to enhance the directivity of the antenna, should it be desired. This would require the proper adjustment of the impedance transformers to maintain proper element excitation.

The response in terms of the impedance BW and 3-dB AR BW (see Figs. 6 and 9, Table II), also makes the proposed array a good candidate for radar and mobile phone charging in the far-field and narrowband WPT retrodirectivity applications based on high-power transmission. In particular, where efficient antenna arrays are required with narrow CP performance with respect to frequency. This type of antenna response is needed to minimize any electromagnetic coupling effects from other sources (acting like a filter) while maintaining CP antenna operation at a single frequency with high power, and also ensuring high radiation efficiency within a compact design. For

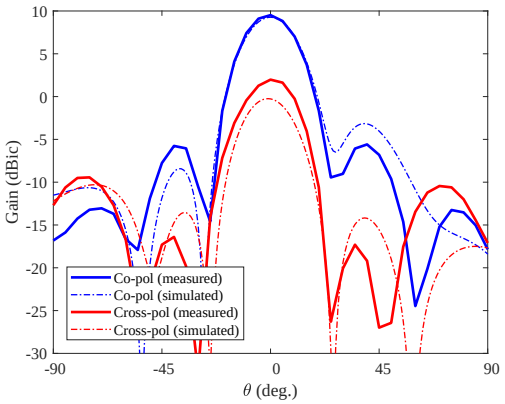

Fig. 10. Realized gain pattern at 2.37 GHz in the x-z-plane (ϕ = 0°).

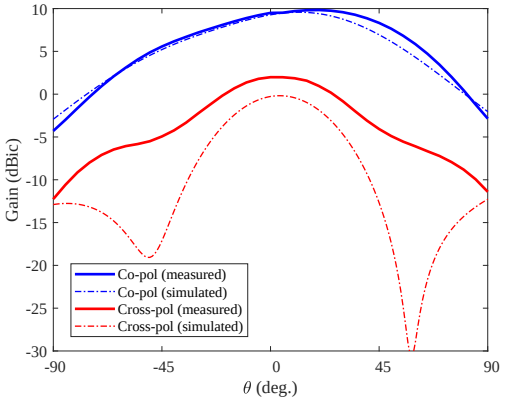

Fig. 11. Realized gain pattern at 2.37 GHz in the y-z-plane (ϕ = 90°).

example, the proposed series-fed array of this work could be an alternative to the arrays used in [26] and [27], which employed a network of series-fed sub-arrays (see Fig. 5 in [26]) to realize a one-dimensional CP retrodirective antenna array. In those works, CP re-radiation of a single-tone and target self-tracking were demonstrated at S-band for mobile phone battery charging and values of over 500 mW of RF power were steered towards the mobile receiver unit at a distance of 0.5 m. However, efficient aperture design for the antennas were not employed since no method to directly control element radiation was considered (i.e. a Chebychev or uniform aperture distribution was not adopted). It is expected that with more efficient and compact arrays, employing a properly designed aperture distribution, as in this work, reduced losses and SLLs are expected in the antenna system. This can support higher levels of single-frequency retrodirected power enabling more proficient WPT.

V. Conclusion

A compact series-fed array design at about 2.4 GHz was proposed in this communication. A high-permittivity substrate, in combination with optimized meander lines, have been used to reduce the size and to provide a high-gain (about 10 dBic) and a circularly polarized beam with a low level for the first sidelobe (below -15 dB). The impact on the performance of the considered single-line feeding network has been accurately analyzed, while the radiation features of the array have been contrasted with the state of the art (see Table II) as reported in the literature. As discussed, no similar compact and single-layer series-fed CP array has been demonstrated with comparable aperture efficiency, uniform excitation of its elements as well as equivalent sidelobe-levels.

Future work could consider the use of more elements or sequential rotation to further enhance the directivity and bandwidth as well

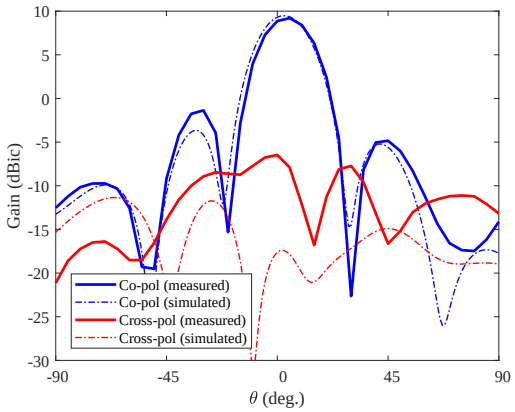

Fig. 12. Realized gain pattern at 2.38 GHz in the x-z-plane ($\phi = 0°$).

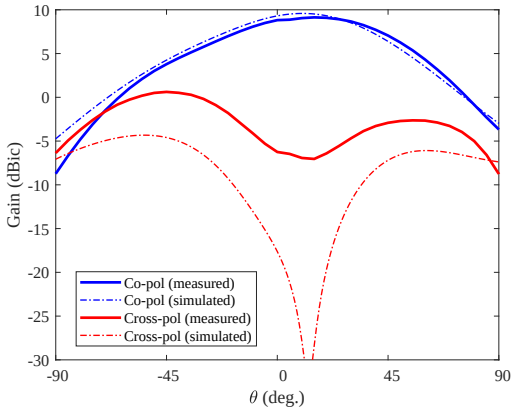

Fig. 13. Realized gain pattern at 2.38 GHz in the y-z-plane ($\phi = 90°$).

as the use of different lumped or distributed components to control the inter-element phasing instead of meander lines. This should be accomplished by minimizing any perturbation to the axial ratio whilst further enhancing design compactness as well as the operating bandwidth as required, or by designing an alternative aperture illumination (other than uniform, such as binomial, Chebychev, or cosine-squared, etc.). Considerations for linear- and dual-polarized implementations are also possible with the developed feeding approach. Furthermore, depending on the constraint on the maximum desired gain, standard windowing procedures could also be considered to achieve lower levels of the first sidelobe as in [28].

REFERENCES

[1] Ramesh Garg, P. Bhartia, I. Bahl, and A. Ittipiboon, *Microstrip Antenna Design Handbook*. Artech House, 2001, ch. 8, p. 524.

[2] K. L. Wong and Y. F. Lin, "Circularly polarised microstrip antenna with a tuning stub," *Electron. Lett.*, vol. 34, no. 9, pp. 831–832, April 1998.

[3] W. S. Chen, C. K. Wu, and K. L. Wong, "Novel compact circularly polarized square microstrip antenna," *IEEE Trans. Antennas Propag.*, vol. 49, no. 3, pp. 340–342, March 2001.

[4] K. Y. Lam, K. Luk, K. F. Lee, H. Wong, and K. B. Ng, "Small circularly polarized U-slot wideband patch antenna," *IEEE Antennas Wirel. Propag. Lett.*, vol. 10, pp. 87–90, 2011.

[5] N. Uddin, Z. N. Chen, and X. Qing, "A compact circularly polarized cross-shaped slotted microstrip antenna," *IEEE Trans. Antennas Propag.*, vol. 60, no. 3, pp. 1584–1588, March 2012.

[6] S. Ogurtsov, S. Koziel, Y. Yu, and Q. S. Cheng, "Design and validation of corporate feeds for lowsidelobe microstrip linear arrays," in *Europ. Conf. Ant. Propag.* IET, 2018, pp. 679–684.

[7] S. Ogurtsov and S. Koziel, "Automated simulation-driven design tuning of circularly polarized microstrip patch antennas," in *IEEE Int. Symp. Antennas Propag.* IEEE, 2016, pp. 569–570.

[8] Q.-Y. Chen, Y.-F. Wei, J.-D. Zhang, and W. Wu, "Dual-band circularly polarized shared-aperture array with wideband and small frequency ratio," in *IEEE Int. Conf. Ubiquitous Wireless Broadband*. IEEE, 2016, pp. 1–3.

[9] S. Koziel, S. Ogurtsov, W. Zieniutycz, and L. Sorokosz, "Simulation-driven design of microstrip antenna subarrays," *IEEE Trans. Antennas Propag.*, vol. 62, no. 7, pp. 3584–3591, 2014.

[10] S. Ogurtsov and S. Koziel, "On alternative approaches to design of corporate feeds for low-sidelobe microstrip linear arrays," *IEEE Trans. Antennas Propag.*, vol. 66, no. 7, pp. 3781–3786, July 2018.

[11] P. Hallbjorner, I. Skarin, K. From, and A. Rydberg, "circularly polarized traveling-wave array antenna with novel microstrip patch element," *IEEE Antennas Wirel. Propag. Lett.*, vol. 6, pp. 572–574, 2007.

[12] S. J. Chen, C. Fumeaux, Y. Monnai, and W. Withayachumnankul, "Dual circularly polarized series-fed microstrip patch array with coplanar proximity coupling," *IEEE Antennas Wirel. Propag. Lett.*, vol. 16, pp. 1500–1503, 2017.

[13] L. Alatan, "Design of a series fed circularly polarized microstrip patch array," in *Proc. IEEE Int. Antennas Prop. Symp.*, vol. 2. IEEE, 2002, pp. 212–215.

[14] S. Karimkashi and G. Zhang, "A dual-polarized series-fed microstrip antenna array with very high polarization purity for weather measurements," *IEEE Trans. Antennas Propag.*, vol. 61, no. 10, pp. 5315–5319, Sep. 2013.

[15] T. Edwards, *Foundations for Microwave Circuit Design*, 4th ed. Wiley, 2016, ch. 9, pp. 236–239.

[16] B. Easter, A. Gopinath, and I. M. Stephenson, "Theoretical and experimental methods for evaluating discontinuities in microstrip," *Radio and Electronic Engineer*, vol. 48, no. 1.2, pp. 73–84, January 1978.

[17] T. R. Cameron, A. T. Sutinjo, and M. Okoniewski, "A circularly polarized broadside scanning patch array," in *Proc. 4th Europ. Conf. Antennas Propag.*, April 2010, pp. 1–3.

[18] ——, "A circularly polarized broadside radiating "herringbone" array design with the leaky-wave approach," *IEEE Antennas Wirel. Propag. Lett.*, vol. 9, pp. 826–829, 2010.

[19] J. Xu, M. Wang, H. Huang, and W. Wu, "Circularly polarized patch array fed by slotted waveguide," *IEEE Antennas Wirel. Propag. Lett.*, vol. 14, pp. 8–11, 2015.

[20] X. Bai, S. Qu, and C. Chan, "Circularly polarized series-fed patch array for THz applications," in *IEEE Int. Symp. Antennas Propag.*, June 2016, pp. 595–596.

[21] K. Wei, J. Li, R. Xu, and G. Yang, "Circularly polarized omnidirectional microstrip antenna array," in *IEEE Int. Symp. Antennas Propag.*, July 2017, pp. 2315–2316.

[22] K. Ito, K. Itoh, and H. Kogo, "Improved design of series-fed circularly polarised printed linear arrays," in *IEE Proceedings Microwaves, Ant. Propag.)*, vol. 133, no. 6. IET, 1986, pp. 462–466.

[23] Y.-H. Yang, J.-L. Guo, B.-H. Sun, Y.-M. Cai, and G.-N. Zhou, "The design of dual circularly polarized series-fed arrays," *IEEE Trans. Antennas Propag.*, vol. 67, no. 1, pp. 574–579, 2019.

[24] B. Ijaz, S. Roy, M. M. Masud, A. Iftikhar, S. Nariyal, I. Ullah, K. Asirvatham, B. Booth, and B. D. Braaten, "A series-fed microstrip patch array with interconnecting CRLH transmission lines for WLAN applications," in *Proc. 7th Europ. Conf. Antennas Propag.*, April 2013, pp. 2088–2091.

[25] T. Kokkinos, A. M. Katsounaros, and A. P. Feresidis, "Series-fed microstrip patch arrays employing metamaterial transmission lines: A comparative study," in *Proc. 2nd European Conf. Antennas Propag.*, Nov 2007, pp. 1–5.

[26] P. D. H. Re, S. K. Podilchak, S. Rotenberg, G. Goussetis, and J. Lee, "Retrodirective antenna array for circularly polarized wireless power transmission," in *Proc. 11th Europ. Conf. Antennas Propag.*, March 2017, pp. 891–895.

[27] P. H. Re, S. Podilchak, S. Rotenberg, G. Goussetis, and J. Lee, "Circularly polarized retrodirective antenna array for wireless power transmission," *IEEE Trans. Antennas Propag.*, (accepted with major revisions, 2019).

[28] C. L. Dolph, "A current distribution for broadside arrays which optimizes the relationship between beam width and side-lobe level," *Proc. IRE*, vol. 34, no. 6, pp. 335–348, June 1946.